Supplemental methods

Enzyme activity assays

Using dounce homogenizers, liver tissues were homogenized in four volumes of reaction buffer (27 mM citrate, 47 mM sodium phosphate dibasic, pH 4.6) containing 5 mg/ml sodium taurocholate. Homogenates were centrifuged at 16,300 x g (4°C) for 15 min and the supernatant was stored at -80°C until further use. Lysosomal enzyme activities were determined using synthetic 4-methylumbelliferyl (4-MU) substrates diluted in reaction buffer. In 96-well black plates, 10 µl sample (serum or liver homogenate) diluted in reaction buffer was mixed with 50 µl of the below 4-MU substrate solutions. α-Gal A activity was measured with 4-MU-α-D-galactopyranoside (4-MU-α-Gal) (Sigma) in the presence of *N*-acetylgalactosamine (GalNAc) (Sigma) (4 mM and 100 mM final concentrations, respectively). GalNAc was used to inhibit α-*N*-acetylgalactosaminidase, an endogenous lysosomal enzyme that also hydrolyzes the 4-MU-α-Gal substrate (1). β-hexosaminidase activity (A and B subunits) was measured with 4-MU-*N*-acetyl-β-glucosaminide (Sigma), and α-mannosidase activity was measured with 4-MU-α-D-mannopyranoside (Research Products International) (1 mM and 2 mM final concentrations, respectively). Reactions were incubated at 37°C for 1 hour and then stopped with 200 µl 0.2 M glycine (pH 10.7). Fluorescence intensities were measured with a BioTek Synergy Mx microplate reader using an excitation of 365 nm and emission of 448 nm. A linear standard curve of 4-methylumbelliferone (sodium salt, Sigma) prepared in 0.2 M glycine (pH 10.7) was used to determine the amount of substrate hydrolyzed. Activity is reported as nmol/h/ml at 37°C (serum) or nmol/h/mg total protein at 37°C (liver homogenate). Total protein concentration was determined using a BCA assay (Thermo Scientific). The limit of detection for α-Gal A was determined to be 2.5 nmol 4-MU.

Isolation of GSLs and TLC

Rat tissue homogenates were prepared by grinding in liquid nitrogen, followed by Dounce homogenization in 50% methanol on ice. The solvent composition was adjusted to

chloroform/methanol/water (30:60:8, *v*/*v*/*v*) and agitated for at least 2 hours at room temperature. The homogenates were then centrifuged to collect precipitated proteins, and the supernatant was kept as lipid extract. The precipitated proteins were re-extracted three times with the same solvent mix, and the original and all three re-extractions were combined and dried under nitrogen gas. For the extraction of plasma GSLs, samples were adjusted to a solvent mixture of chloroform/methanol/water (30:60:8, *v*/*v*/*v*), and following agitation, centrifuged to precipitate proteins. The supernatant was kept as lipid extract, and the protein pellet was extracted three times with the same solvent mix. All supernatants were combined. For RBC GSLs, pelleted RBCs were first suspended in twice the pellet volume of 50% MeOH to avoid aggregation and then sonicated for 3 min. The solvent mixture was then adjusted to chloroform/methanol/water (4:8:3, *v*/*v*/*v*). The extract was agitated and then centrifuged to collect precipitated proteins. The precipitated material was re-extracted twice with chloroform/methanol/water (30:60:8, *v*/*v*/*v*) and all supernatants were combined. Contaminating glycerophospholipids were removed from the dried lipid extract by saponification. Briefly, 0.5 M potassium hydroxide in methanol was incubated with the dried extract for at least 6 h at 37°C. The saponification reaction was terminated with an equal volume of 5% acetic acid to make the final solution 50% aqueous in methanol. GSLs were desalted and separated from released fatty acids on tC18 Sep-Pak cartridges (Waters) pre-equilibrated with methanol and 1% acetic acid. GSLs were analyzed by separation on HPTLC silica gel 60 plates (EMD Millipore) using a mobile phase of chloroform/methanol/water (solvent systems are specified in figure legends) and visualized by spraying with 0.25% orcinol (Sigma) in 3 M aqueous H_2SO_4/ethanol (1:1, *v*/*v*). Standards of neutral GSLs and gangliosides were obtained from Matreya LLC. Serum GSL abundance was normalized to serum volume, DRG GSL was normalized to mg wet tissue weight, and RBC and brain GSLs were normalized to mg dried, delipidated protein.

Exoglycosidase digestions

α-Galactosidase from green coffee beans and β-galactosidase from bovine testes and Aspergillus oryzae were used to cleave the terminal galactose residues of GSLs. Both exoglycosidases were obtained

from Sigma, and digestions of GSLs were performed as follows. For α-galactosidase treatment, GSLs were digested in 50 µl of 100 mM phosphate-citrate buffer, pH 6.5 at 25 °C in the presence of γ-galactonolactone (0.5 mg/ml). For β-galactosidase treatments, GSLs were digested in 50 µl of 20 mM phosphate-citrate buffer, pH 4.5 at 30°C (Aspergillus oryzae) or 100 mM phosphate-citrate buffer, pH 4.3 at 37°C (bovine testis), respectively. All digestions were carried out in the presence of 0.1 mg/ml of sodium taurodeoxycholate. The reaction mixture was desalted by Folch's partition prior to subsequent TLC and MS analyses. GSLs were fractionated using Iatrobeads 6RS-8060 (Iatron Laboratories Inc.).

Mass spectrometry of GSLs

Approximately 1-3 µg of tC18-purified GSLs were permethylated with ^{12}C-methyliodide prior to MS analysis according to the method of Anumula and Taylor (2). Known amounts of a maltotetraose oligosaccharide (Dp4) were permethylated with ^{13}C-methyliodide for use as reference standards for GSL quantification (3). Permethylated GSLs were reconstituted in methanol/2-propanol/1-propanol/water (16:3:3:2 by volume) containing 1 mM NaOH for direct infusion into the mass spectrometer. Ten picomoles of ^{13}C-permethylated maltotetraose standard (Dp4) were spiked into permethylated GSL samples, and the mixture was analyzed by direct infusion into a linear ion trap mass spectrometer (LTQ; Thermo Fisher Scientific, Waltham, MA) using a nanoelectrospray source at a syringe flow rate of 0.4-0.6 µL/min and capillary temperature set to 210°C (4-6). The instrument was tuned with a mixture of permethylated GSLs and Dp standards in positive ion mode. For fragmentation by collision-induced dissociation (CID) in MS/MS and MS^n, a normalized collision energy of 35% to 40% was used.

Detection and absolute quantification of the prevalence of individual GSLs was accomplished using the total ion mapping (TIM) and neutral loss scan (NL scan) functionalities of the Xcalibur software package version 2.0 (Thermo Fisher Scientific) as previously described (5, 7). Briefly, for TIM, the *m/z* range from 600 to 2000 was automatically scanned in successive 2.8 mass unit windows with a window-to-window overlap of 0.8 mass units, which allowed the naturally occurring isotopes of each GSL species to be summed into a single response, thereby increasing detection sensitivity. Most GSLs were identified

as singly, doubly, and triply charged, sodiated species [M+Na] in positive mode. Peaks for all charge states were deconvoluted by the charge state and summed for quantification. For NL scans, an MS workflow was defined in which the highest intensity peak detected by full MS was subjected to CID fragmentation. The major MS/MS fragment ions produced by CID of GSL preparations correspond to the neutral loss of the ceramide moiety, leaving an intact GSL oligosaccharide ion for subsequent fragmentation in MS^n. Therefore, a NL scan workflow was designed to acquire MS^n fragmentation if an MS/MS profile contained a fragment ion with an *m/z* equivalent to loss of the most prevalent ceramide moiety. Following this data-dependent acquisition, the workflow returned to the full MS, excluded the parent ion just fragmented, and chose the peak of next highest intensity for the same MS/MS and MS^n analysis. By this data-dependent acquisition workflow, GSL glycan profiles and MS^n sequencing were rapidly acquired for complex mixtures of GSLs (7). Permethylated GSLs were analyzed from multiple biological replicates for serum, RBC, DRG, and brain tissue (n = 3 for WT and n = 3 for KO). For all samples, GSLs were characterized by MS and by TLC. The MS-based glycomics data generated in these analyses and the associated annotations are presented in accordance with the MIRAGE standards and the Athens Guidelines (8, 9).

Optimization of lyso-GSL analysis

The free amino group in the sphingoid base of lyso-GSLs significantly suppresses ionization in the mass spectrometer, thereby decreasing detection sensitivity. We permethylate prior to analysis because this derivatization provides in-depth structural information and increased ionization efficiency for MS^n analysis. However, permethylation of molecules with a free amino group results in the formation of quaternary ammonium salts that suppress ionization. To circumvent this problem, we developed an improved approach for the structural assignment of lyso-GSL species using a one-step chemical reaction that results in N-acetylation of the sphingoid base. We validated this method using commercially obtained, synthetic lyso-Gb3. Following permethylation of the synthetic lyso-Gb3, the product was subjected to N-acetylation with anhydrous acetic acid in pyridine. The resulting N-acetylated, O-

permethylated lyso-Gb3 demonstrated 2-fold stronger signal than its non-acetylated form. We also noticed that the permethylated lyso-Gb3, without N-acetylation, did not produce signature CID ions corresponding to glycan fragmentation, most likely due to impaired formation of metal adduct [M+Na]+. However, the N-acetylated, O-permethylated form of lyso-Gb3 efficiently formed sodiated adducts and productively fragmented by CID to give glycan signature ions, allowing effective quantification by reference to the permethylated MS standard. For the detection of lyso-GSL species in rat materials, TIM profiles were filtered with neutral loss of C18-sphingoshine (Δ mass, 351 (1+)) to evaluate the expression of lyso-GSL species.

Protein-linked glycan analysis

N-glycans were released from rat glycoproteins by PNGaseF digestion and permethylated as described previously (5). Briefly, glycoproteins were digested with trypsin and chymotrypsin (Sigma), and glycopeptides were enriched from the digests by Sep-Pak C18 cartridge chromatography (Waters). Following release by PNGaseF (NEB), N-glycans were permethylated prior to analysis. Permethylated N-glycans were analyzed by NSI-MS in positive ion mode and quantified relative to a known amount of external standard (maltotetraose, Dp4, permethylated with heavy methyliodide) supplemented into the sample prior to injection. For the characterization of sulfated N-glycans, TIM profiles were filtered with neutral loss of sulfate group (-OSO3Na). N-glycan structures carrying the sulfate group were further subjected to manual MS^n analysis for complete structural determination.

Behavior assays

Rats were acclimated in a plastic box placed over 6.35 × 6.35 mm wire mesh for at least 25 min. von Frey filaments (Bioseb) were applied to the plantar surfaces of hind paws, and mechanical thresholds were measured by the up-down method (10, 11). Mechanical sensitivity in rats was also assessed using a supratheshold stimulus of 86 mN (8.8 g, filament 13), where the von Frey filament was applied 10 times to the glabrous skin of the hindpaw and the number of stimulus-evoked responses was recorded. The

needle method was used to determine sensitivity to sharp punctate force (12, 13). The spinal anesthesia needle was applied 10 times to each plantar surface and the percent response (paw stomping, lifting, licking) was recorded. The dry ice method was used to measure cold sensitivity (14). Rats were acclimated for at least 25 min in a plastic cage placed over an elevated sheet of tempered glass (3.18 mm thick). Compressed dry ice was applied to the plantar hind paw via a 3 ml plastic syringe with the hub placed flush with the bottom of the glass, and the time to reaction (stomping, shaking, moving, or lifting of the foot) was measured. Each paw was probed four times in a single session (eight technical replicates total per rat), with 15 min pause between sequential tests on each foot. The Hargreaves test to measure heat sensitivity (15), where a radiant heat source was directed at the rat hind paw. Rats were given at least 24 hours of rest between each behavioral assay. In both the dry ice and Hargreaves tests, the stimulus was removed at 20 s if there was no response to avoid damaging tissue. TRPA1 inhibitor HC-030031 (Sigma H4415) treatment during behavioral testing was performed by subcutaneously injecting 300 µg in 50 µl vehicle (PBS with 0.5% DMSO and 0.25% polysorbate 80) into the hind paw one hour prior to behavioral testing. All behavior assays were performed as described above. Throughout the experiment, the experimenter was blinded to the genotype and treatment.

Patch-clamp electrophysiology

A perfusion chamber containing DRG neurons above a Nikon Eclipse TE200 inverted microscope was assembled and was continuously superfused with an extracellular HEPES solution containing: 140 mM NaCl, 5 mM KCl, 2 mM $CaCl_2$,1mM $MgCl_2$,10mM HEPES, and 10mM glucose, pH 7.4 ± 0.03, and 310 ± 3 mOsm. Neurons < 32 µm were patched in voltage clamp mode (-70 mV) with borosilicate glass pulled pipettes (Sutter Instrument Company, Novato, CA) filled with intracellular normal HEPES solution containing: 135 mM KCl, 10 mM NaCl, 1 mM $MgCl_2$, 1 mM EGTA, 0.2 mM NaGTP, 2.5 mM ATP-Na_2, and 10 mM HEPES, pH 7.20 ± 0.05, and 290 ± 3 mOsm. For all cells, cell capacitance and series resistance were kept below 10 MΩ and leak currents < 300 pA. In current clamp

mode, stepwise square pulses were used to elicit the first action potential (rheobase). In voltage clamp mode, and cells were mechanically stimulated using a 1-2 μm tip borosilicate glass pipette driven by a piezo stack actuator (PA25, PiezoSystem) with a velocity of 106.25 μm/ms. Mechanical stimulation of cells was done by increasing displacements in ~0.84 μm increments (1.68 μm/V) for 200 ms. A one minute break was given between each pipette displacement in order to avoid sensitization/desensitization of the neuron. Recordings were made using an EPC9 amplifier (HEKA Electronics) and Pulse software (HEKA Electronics). Data analysis was performed with FitMaster (HEKA Electronics). Each mechanically induced inward current was fitted onto a monoexponential decay equation and the time of inactivation constant (τ) was noted. Neurons were classified as mechanically insensitive if they did not respond to focal mechanical probing with an inward current amplitude of 20 pA to at least 4 stimulations. The experimenter was blinded to genotype throughout the experiment and analysis.

Supplemental figures and legends

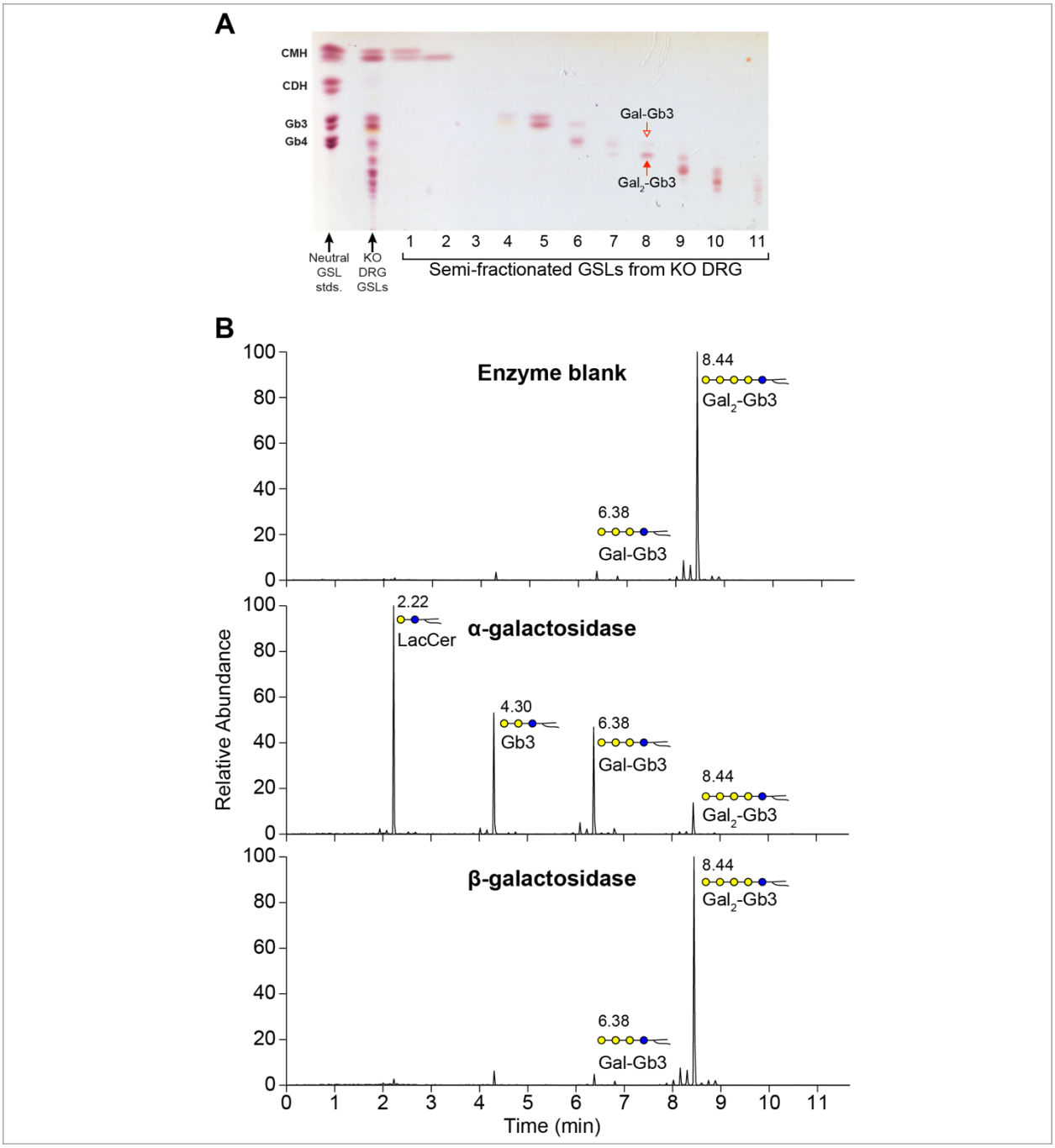

Figure S1. Exogalactosidase digestion demonstrates α-linked galactose extension on KO dorsal root ganglia (DRG) glycosphingolipids (GSLs). DRG GSLs were fractionated by Iatrobeads silica column chromatography (0.5 cm x 8 cm). The column was equilibrated with chloroform/methanol/water (90:10:1, *v/v/v*). DRG GSLs were loaded and eluted step-wise with three bed volumes of each chloroform/methanol/water solvent mixture as follows: 90:10:1, 80:20:1, 70:30:2, 60:40:3, 50:50:5 and 20:80:10, *v/v/v*. Fractions of 1.5 ml volume were collected and an aliquot of each was monitored by TLC, developed in chloroform/methanol/water (60:40:10, *v/v/v*) and sprayed with orcinol-H_2SO_4 reagent for

glycan detection. (**A**) Based on orcinol staining, the Iatrobead fractions were combined into eleven pools. Fraction 8 was confirmed to be highly enriched in ceramide pentasaccharides (CPS) by TLC analysis and subsequent mass spectrometry analysis. (**B**) CPS was treated with α-galactosidase from green coffee beans, β-galactosidase from bovine testes, and no enzyme control (buffer alone), as described in Methods. The products of the reaction mixture were permetheylated and subjected to total ion mapping (TIM) analysis by nanospray ionization-mass spectrometry. CPS was sensitive to α-galactosidase digestion, resulting in the detection of the degradation products monogalactosyl-Gb3, Gb3, and LacCer (middle TIM profile). In contrast, CPS was resistant to β-galactosidase (bottom TIM profile), confirming that Gb3 is extended with α-galactose residues in the Fabry rat model. Abbreviations: ceramide monohexoside (CMH), ceramide dihexoside (CDH), lactosylceramide (LacCer), globotriaosylceramide (Gb3), globotetraosylceramide (Gb4), Gb3 with a single galactose extension (Gal-Gb3), Gb3 with two galactose extensions (Gal_2-Gb3).

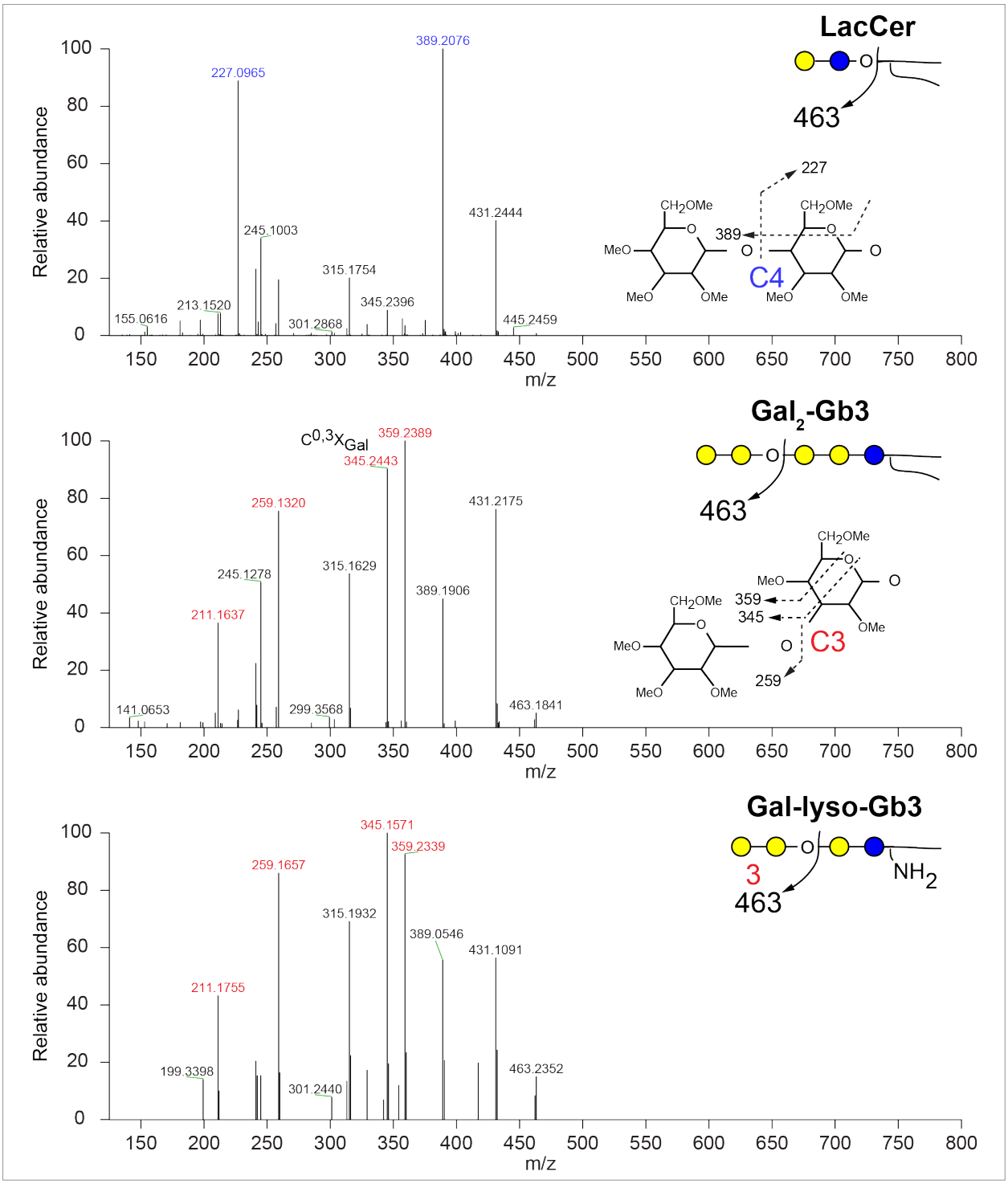

Figure S2. Nanospray ionization-mass spectrometry (NSI-MS^n) fragmentation places terminal galactose extension at 3-position on polygalactosylated glycosphingolipids (GSLs) isolated from KO dorsal root ganglia (DRGs). In order to characterize the linkage position of the terminal galactose on galactosylated Gb3 species, MS^n analysis was performed on Gal$_2$-Gb3 and Gal-lyso-Gb3 (middle panel and bottom panel, respectively). MS^n fragmentation of LacCer (galactose1-4glucose-ceramide) is presented (top panel) as a reference to demonstrate detection of C4-linked galactose for comparison to the

bottom two panels. All three GSL species produce a fragment ion at m/z 463 that corresponds to a disaccharide which can be subjected to further collision-induced dissociation fragmentation. MS^n of the m/z 463 fragment derived from the LacCer standard generated smaller fragments at m/z 227 and 389, which correspond to sodiated form of internal galactose and cross-ring $C^{0,4}X_{Gal}$, respectively, and place the galactose substitution at the 4 position of the glucose residue. In contrast, MS^n fragmentation patterns derived from mono- and di-galactosylated Gb3 species are different from the LacCer fragmentation pattern. MS^4 fragments at m/z 259, 345, and 359, which correspond to sodiated form of terminal galactose and the cross-rings $C^{0,3}X_{Gal}$ and $^{1,4}A_{Gal}$, respectively, place the terminal galactose residue at the 3 position of the subterminal galactose residue in mono- and di-galactosylated Gb3 (bottom and middle panels, respectively). Abbreviations: lactosylceramide (LacCer), globotriaosylceramide (Gb3), Gb3 with two galactose extensions (Gal_2-Gb3), globotriaosylsphingosine (lyso-Gb3), lyso-Gb3 with a single galactose extension (Gal-lyso-Gb3).

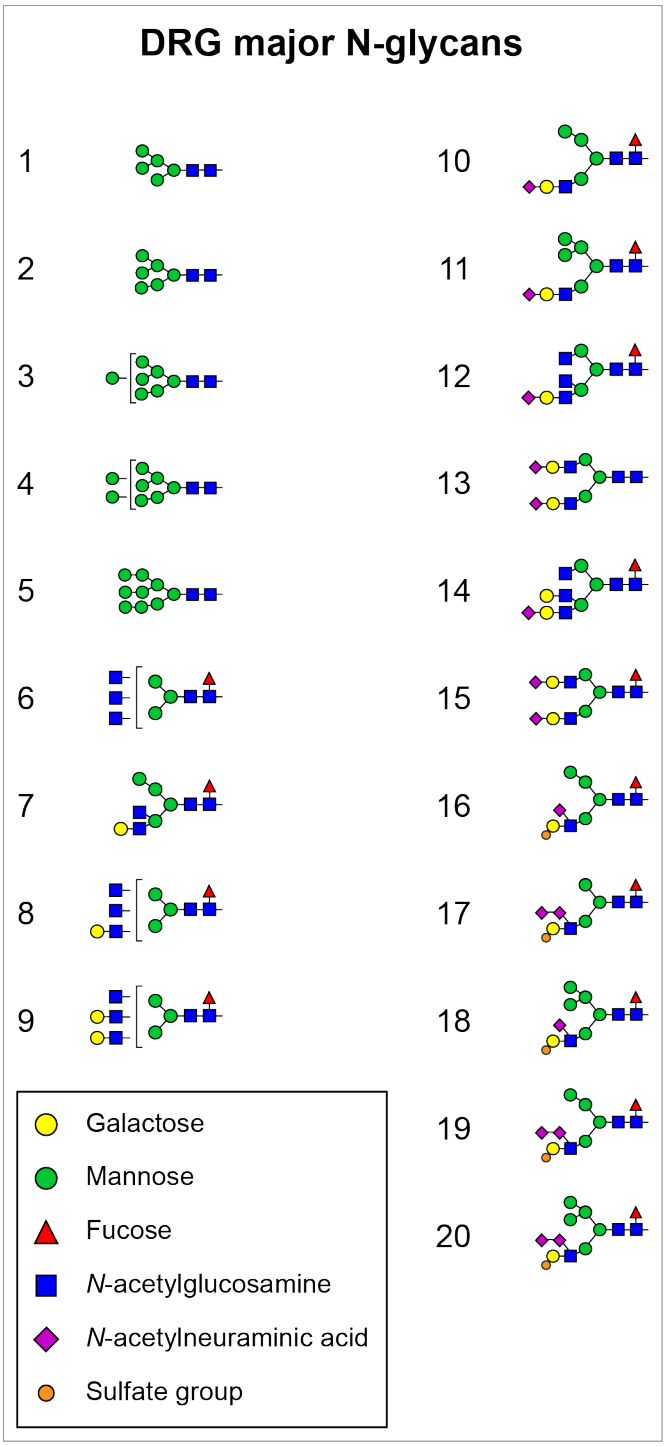

Figure S3. Glycans detected in WT and KO dorsal root ganglia (DRGs). N-linked glycans released from DRG proteins (annotated in **Figure 5**) are shown as Symbol Nomenclature for Glycans representations. The structures of these 20 glycans were validated by nanospray ionization-mass spectrometry as necessary to identify and localize specific features, including sulfation and disialylation.

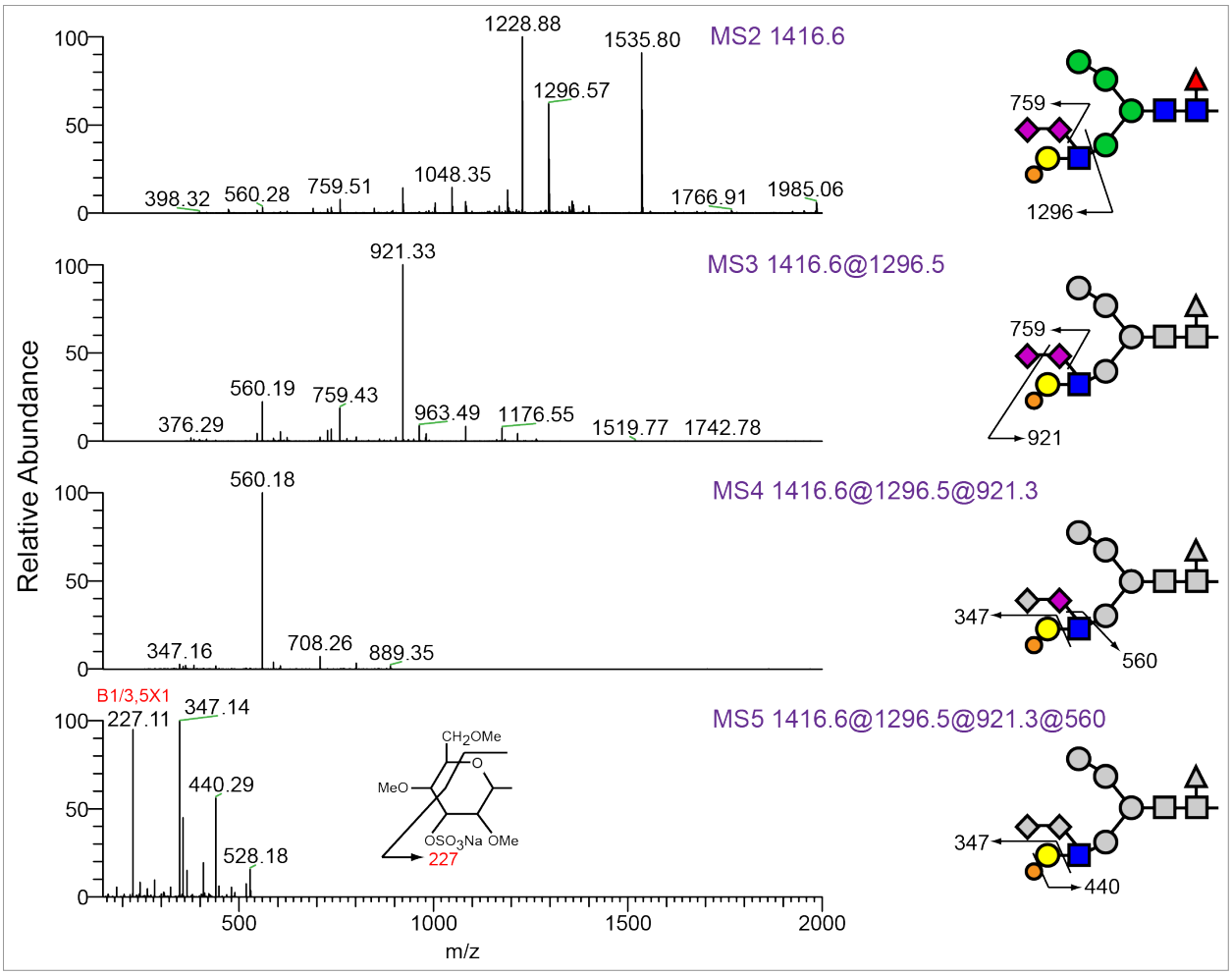

Figure S4. Nanospray ionization-mass spectrometry (NSI-MS^n) fragmentation places sulfate and disialyl modifications on the *N*-acetyllactosamine (LacNAc) extension of a hybrid N-glycan. Structure #19 (see **Figure S3** and **Table S1**), observed at m/z 1416, was detected in WT but reduced in KO dorsal root ganglia. The topology of the glycan was revealed by MS^n collision-induced dissociation fragmentation. Sequential fragmentation produced a unique MS^2 fragment ion at m/z 1296, which demonstrates the presence of a monosulfated and disialylated LacNAc epitope. Further MS^n analysis generated an MS^4 ion at m/z 347 which places the sialic acids on the subterminal *N*-acetylglucosamine (GlcNAc) and an MS^5 cross-ring fragment which confirmed that the sulfate was at the C3-position of the terminal galactose.

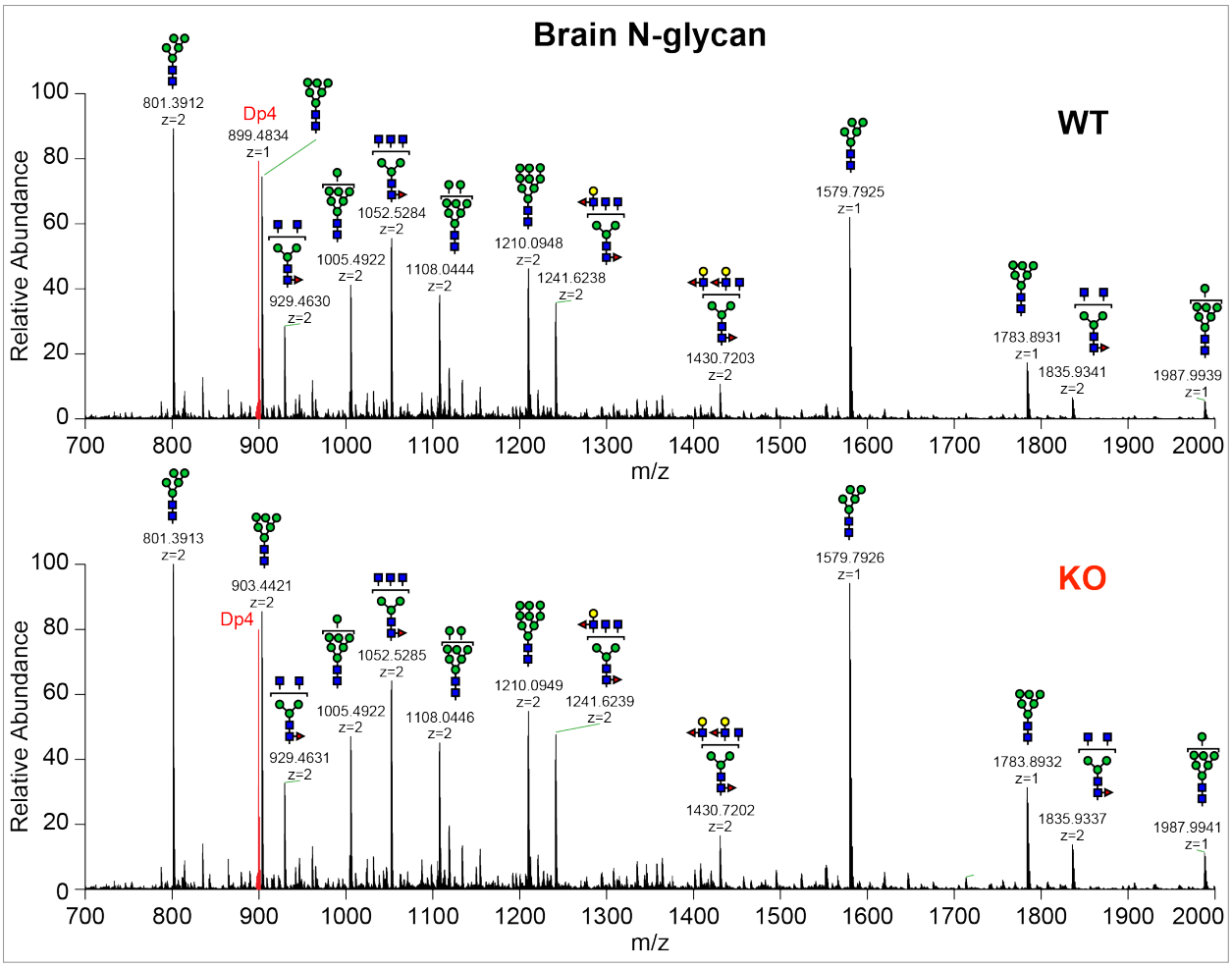

Figure S5. Full mass spectrometry profiles of rat brain N-glycans. Rat brain N-glycans released from tryptic glycopeptides were permethylated and analyzed by nanospray ionization-mass spectrometry in positive ion mode. Permethylated maltotetraose (Dp4) was used as reference standard. High mannose type and triantennary glycans were the most abundant structures in both WT and KO rat brains.

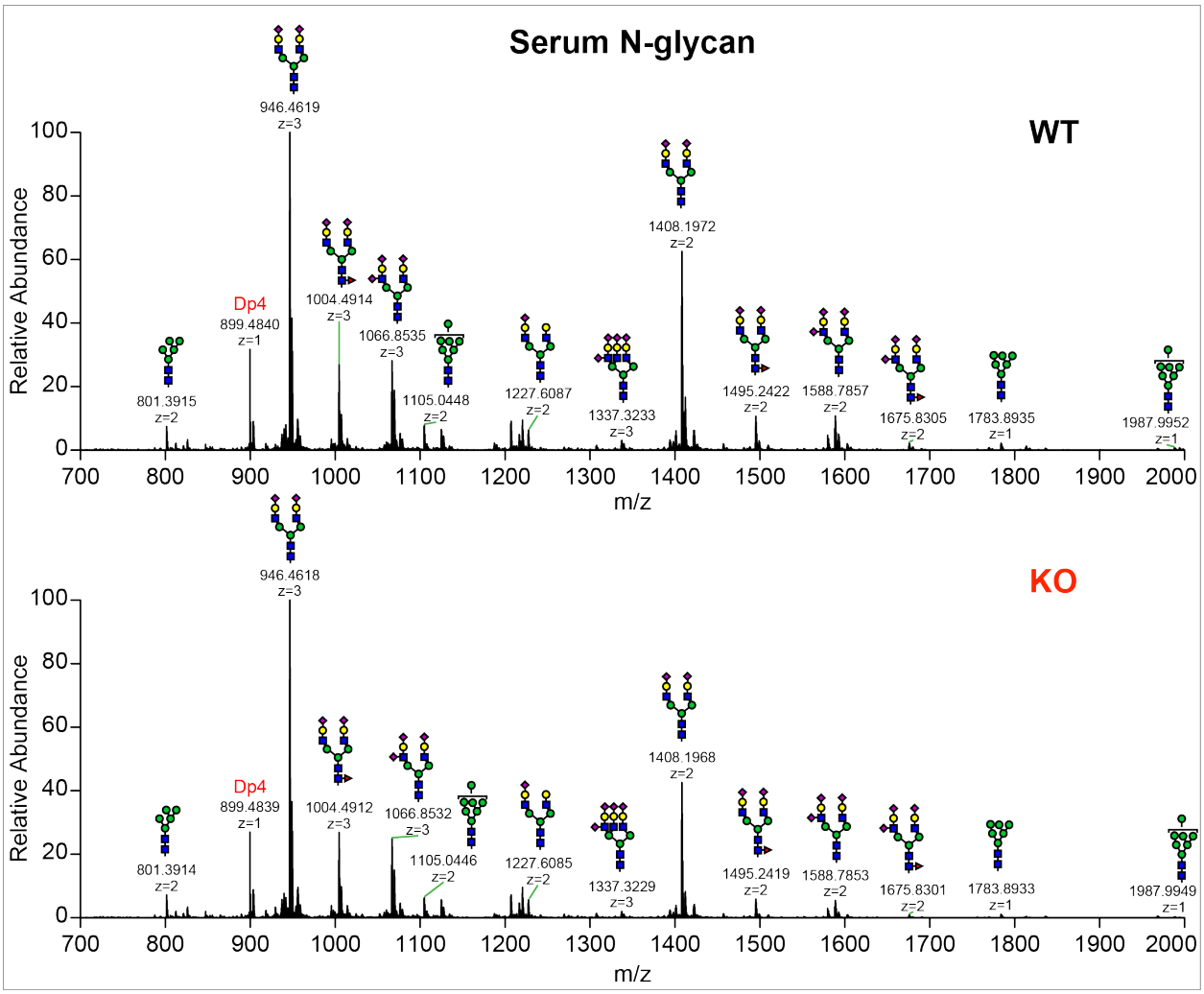

Figure S6. Full mass spectrometry profiles of rat serum N-glycans. Rat serum N-glycans released from tryptic glycopeptides were permethylated and analyzed by nanospray ionization-mass spectrometry in positive ion mode. Complex, biantennary glycans fully modified with sialic acid on both arms were the most abundant structures in WT and KO rat serum.

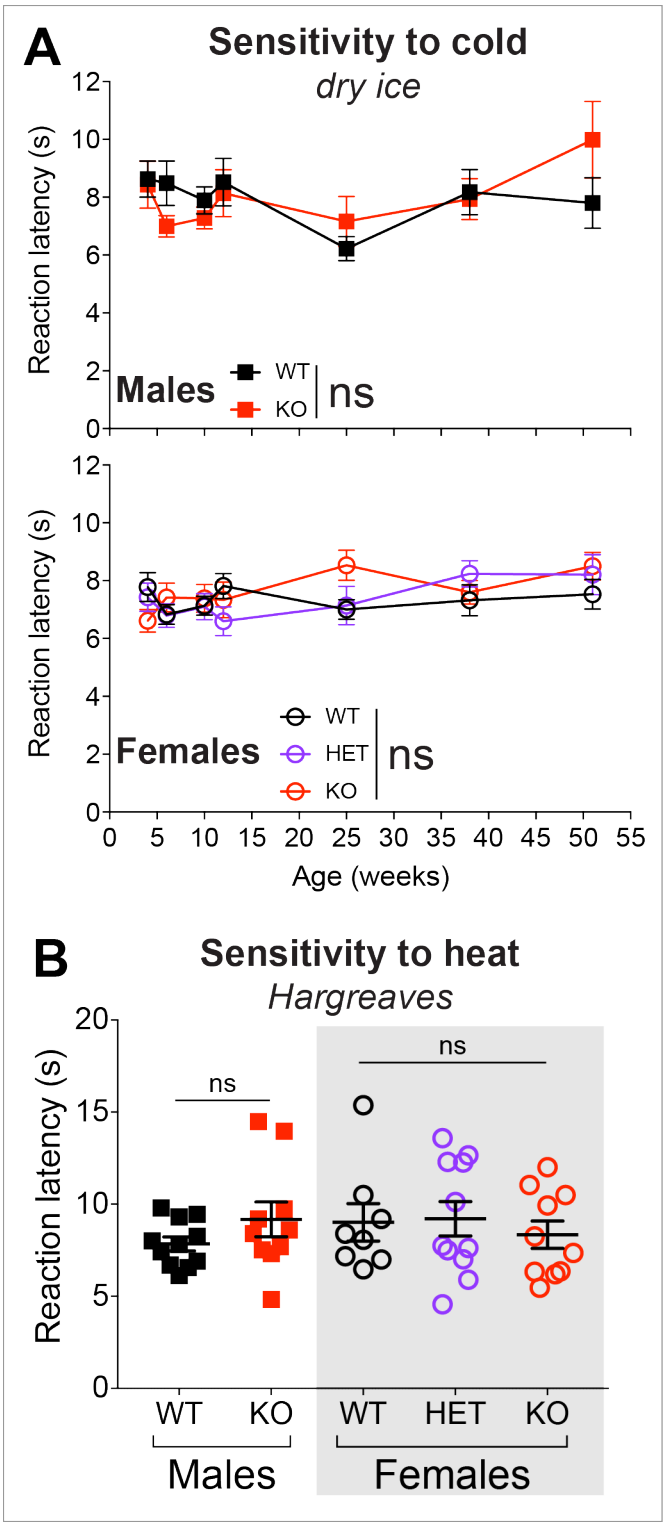

Figure S7. Fabry rats between 4 weeks and 1 year of age do not show behavioral differences to thermal stimuli. (**A**) Rat hind paws were probed with compressed dry ice and reaction latency was recorded. Four dry ice applications per paw were applied in a single session to each rat. Time points included 4, 6, 10, 12, 25, 38, and 51 weeks. (**B**) Hargreaves data from rats at 52 weeks of age. A radiant heat source was directed at rat hind paws and reaction latency was measured. Left and right paws were

subjected to the heat source eight times each, and the mean of these applications is shown in each data point (each representing a biological replicate). Panels (**A**) and (**B**) include data from ≥ 8 rats of each genotype, and the exact numbers of biological replicates in panel (**A**) are given in **Table S5**. Shown are mean ± SEM. Sensitivity to cold data (**A**) was analyzed with a two-way ANOVA. Sensitivity to heat data (**B**) was analyzed with an unpaired, two-tailed t-test (males, unshaded) or a one-way ANOVA (females, shaded).

Table S1. Mass parameters for permethylated, N-linked glycans detected in dorsal root ganglia

Glycan Class	Glycan #	Composition	Theoretical Mass	Observed Mass	*m/z*	Deconvoluted Mass
High-Man glycans	1	M5N2	801.387	801.387	2	1579.794
	1	M5N2	1579.783	1579.783	1	1579.793
	2	M6N2	903.436	903.436	2	1783.892
	2	M6N2	1783.882	1783.882	1	1783.892
	3	M7N2	1005.486	1005.487	2	1987.994
	3	M7N2	1987.982	1987.982	1	1987.992
	4	M8N2	1107.536	1107.535	2	2192.090
	5	M9N2	1209.586	1209.586	2	2396.192
Non-sialylated glycans	6	N3M3N2F	1052.020	1052.021	2	2081.062
	7	Gal1N2M4N2F1	1133.557	1133.557	2	2244.134
	8	Gal1N3M3N2F1	1154.070	1154.071	2	2285.162
	9	Gal2N3M3N2F1	1256.120	1256.120	2	2489.260
Sialylated glycans	10	SA1Gal1N1M4N2F1	802.050	802.050	3	2360.181
	10	SA1Gal1N1M4N2F1	1191.581	1191.581	2	2360.182
	11	SA1Gal1N1M5N2F1	870.083	870.418	3	2565.285
	11	SA1Gal1N1M5N2F1	1293.630	1293.631	2	2564.282
	12	SA1Gal1N3M3N2F1	1334.657	1334.658	2	2646.336
	13	SA2Gal2N2M3N2	946.120	946.121	3	2792.394
	13	SA2Gal2N2M3N2	1407.686	1407.686	2	2792.392
	14	SA1Gal2N3M3N2F1	1436.707	1436.707	2	2850.434
	15	SA2Gal2N2M3N2F1	1004.150	1004.150	3	2966.481

	15	SA2Gal2N2M3N2F1	1494.731	1494.731	2	2966.482
Sulfated	16	S1SA1Gal1N1M4N2F1	831.358	831.358	3	2448.105
and	16	S1SA1Gal1N1M4N2F1	1235.542	1235.543	2	2448.106
sialylated	17	S1SA2Gal1N1M3N2F1	1314.142	1314.142	2	2605.304
glycans	18	S1SA1Gal1N1M5N2F1	1337.592	1337.596	2	2652.212
	19	S1SA2Gal1N1M4N2F1	951.749	951.750	3	2809.281
	19	S1SA2Gal1N1M4N2F1	1416.129	1416.132	2	2809.284
	20	S1SA2Gal1N1M5N2F1	1019.782	1019.783	3	3013.379
	20	S1SA2Gal1N1M5N2F1	1518.179	1518.179	2	3013.358

1 Abbreviations for monosacchride compostion are as follows: M, mannose; N, *N*-acetylglucosamine; Gal,
2 galactose; F, fucose; SA, sialic acid; S, sulfate. Charge state is given as *m/z*.

Table S2. Statistical analysis of sensitivity to noxious force behavioral data

Comparison	p-value
Within a genotype (4 vs 51 weeks)	
WT males	****
KO males	****
WT females	ns
HET females	****
KO females	****
At 51 weeks	
WT vs KO males	****
WT vs HET females	ns
WT vs KO females	****
HET vs KO females	****
At 4 weeks	
WT vs KO males	ns
WT vs HET females	*
WT vs KO females	ns
HET vs KO females	ns

Statistical significance was determined using a chi-square test; HET = heterozygous.

Table S3. Mechanical thresholds (von Frey test) biological replicates

Age (weeks)	WT males	KO males	WT females	HET females	KO females
10	15	9	11	9	11
12	10	8	11	9	8
25	9	10	8	8	8
38	9	10	9	10	8
51	8	8	10	8	8

Table S4. Sensitivity to noxious sharp force (needle test) biological replicates

Age (weeks)	WT males	KO males	WT females	HET females	KO females
4	10	11	8	8	11
6	10	9	11	9	11
10	14	9	8	8	11
12	11	8	8	8	8
25	8	8	8	8	8
38	9	10	9	10	8
51	8	8	10	8	8

Table S5. Sensitivity to cold (dry ice test) biological replicates

Age (weeks)	WT males	KO males	WT females	HET females	KO females
4	10	11	8	8	11
6	10	9	11	9	11
10	16	9	8	8	11
12	11	8	8	8	8
25	8	8	8	8	8
38	9	10	9	10	8
51	8	8	10	8	8

Supplemental References

1. Mayes JS, Scheerer JB, Sifers RN, and Donaldson ML. Differential assay for lysosomal alpha-galactosidases in human tissues and its application to Fabry's disease. *Clin Chim Acta.* 1981;112(2):247-51.
2. Anumula KR, and Taylor PB. A comprehensive procedure for preparation of partially methylated alditol acetates from glycoprotein carbohydrates. *Anal Biochem.* 1992;203(1):101-8.
3. Mehta N, Porterfield M, Struwe WB, Heiss C, Azadi P, Rudd PM, et al. Mass Spectrometric Quantification of N-Linked Glycans by Reference to Exogenous Standards. *J Proteome Res.* 2016;15(9):2969-80.
4. Vukelic Z, Zamfir AD, Bindila L, Froesch M, Peter-Katalinic J, Usuki S, et al. Screening and sequencing of complex sialylated and sulfated glycosphingolipid mixtures by negative ion electrospray Fourier transform ion cyclotron resonance mass spectrometry. *J Am Soc Mass Spectrom.* 2005;16(4):571-80.
5. Aoki K, Perlman M, Lim JM, Cantu R, Wells L, and Tiemeyer M. Dynamic developmental elaboration of N-linked glycan complexity in the Drosophila melanogaster embryo. *J Biol Chem.* 2007;282(12):9127-42.
6. Nimrichter L, Burdick MM, Aoki K, Laroy W, Fierro MA, Hudson SA, et al. E-selectin receptors on human leukocytes. *Blood.* 2008;112(9):3744-52.
7. Boccuto L, Aoki K, Flanagan-Steet H, Chen CF, Fan X, Bartel F, et al. A mutation in a ganglioside biosynthetic enzyme, ST3GAL5, results in salt & pepper syndrome, a neurocutaneous disorder with altered glycolipid and glycoprotein glycosylation. *Hum Mol Genet.* 2014;23(2):418-33.
8. Wells L, Hart GW, and Athens Guidelines for the Publication of Glycomics D. Glycomics: building upon proteomics to advance glycosciences. *Mol Cell Proteomics.* 2013;12(4):833-5.

9. York WS, Agravat S, Aoki-Kinoshita KF, McBride R, Campbell MP, Costello CE, et al. MIRAGE: the minimum information required for a glycomics experiment. *Glycobiology.* 2014;24(5):402-6.

10. Chaplan SR, Bach FW, Pogrel JW, Chung JM, and Yaksh TL. Quantitative assessment of tactile allodynia in the rat paw. *J Neurosci Methods.* 1994;53(1):55-63.

11. Dixon WJ. Efficient analysis of experimental observations. *Annu Rev Pharmacol Toxicol.* 1980;20:441-62.

12. Hogan Q, Sapunar D, Modric-Jednacak K, and McCallum JB. Detection of neuropathic pain in a rat model of peripheral nerve injury. *Anesthesiology.* 2004;101(2):476-87.

13. Moehring F, O'Hara CL, and Stucky CL. Bedding Material Affects Mechanical Thresholds, Heat Thresholds, and Texture Preference. *J Pain.* 2016;17(1):50-64.

14. Brenner DS, Golden JP, and Gereau RWt. A novel behavioral assay for measuring cold sensation in mice. *PLoS One.* 2012;7(6):e39765.

15. Hargreaves K, Dubner R, Brown F, Flores C, and Joris J. A new and sensitive method for measuring thermal nociception in cutaneous hyperalgesia. *Pain.* 1988;32(1):77-88.